Research Paper

Cyanobacteria blooms induce embryonic heart failure in an endangered fish species

Jinmei Zi[a], Xiaofu Pan[b], Hugh J. MacIsaac[c,a], Junxing Yang[b], Runbing Xu[a], Shanyuan Chen[a], Xuexiu Chang[a,*]

[a] *School of Ecology and Environmental Sciences, Yunnan University, Kunming 650091, PR China*
[b] *Kunming Institute of Zoology, Chinese Academy of Sciences, Kunming 650223, PR China*
[c] *Great Lakes Institute for Environmental Research, University of Windsor, Windsor, ON N9 B 3P4, Canada*

ABSTRACT

Cyanobacterial blooms drive water-quality and aquatic-ecosystem deterioration in eutrophic lakes worldwide, mainly owing to their harmful, secondary metabolites. The response of fish exposed to these cyanobacterial chemicals, however, remains largely unknown. In this paper, we employed an endangered fish species (*Sinocyclocheilus grahami*) in Dianchi Lake, China to evaluate the risks of cell-free exudates (MaE) produced by a dominant cyanobacterium (*Microcystis aeruginosa*) on embryo development, as well as the molecular mechanisms responsible. MaE (3d cultured) caused a reduction of fertilization (35.4%) and hatching (15.5%) rates, and increased mortality rates ($\leq$90.0%) and malformation rate (27.6%), typically accompanied by heart failure. Proteomics analysis revealed that two greatest changed proteins – protein S100A1 (over-expressed 26 times compared with control) and myosin light chain (under-expressed 25 fold) – are closely associated with heart function. Further study revealed that heart failure was due to calcium ion imbalance and malformed cardiac structure. We conclude that harmful secondary metabolites from cyanobacteria may adversely affect embryo development in this endangered fish, and possibly contribute to its disappearance and unsuccessful recovery in Dianchi Lake. Hazardous consequences of substances released by cyanobacteria should raise concerns for managers addressing recovery of this and other imperiled species in affected lakes.

1. Introduction

Cyanobacteria blooms are increasing in frequency on a worldwide basis, with further increases predicted in association with climate change (Gong et al., 2017; Visser et al., 2016; Paerl et al., 2014; Paerl and Paul, 2012). Cyanobacterial blooms have been reported on every continent except Antarctica, encompassing 108 countries (Harke et al., 2016). Blooms increase turbidity, destroy aquatic plants, and alter fish habitats. Some cyanobacteria produce toxins, which can cause serious human liver and renal damage, as well as neurological and skin diseases (Harke et al., 2016; Testai et al., 2016; Barda et al., 2015), and present health risks to livestock or wildlife that drink or use contaminated water (Bengis et al., 2016; Lopez-Rodas et al., 2008; Stewart et al., 2008). Cyanobacteria thus threaten many of the world's major aquatic ecosystems including Lake Victoria in Africa, Lake Erie in North America, the Baltic Sea in Europe, and lakes Taihu and Dianchi in China (Paerl, 2008). In one high profile case, the Lake Erie water supply for Toledo, Ohio was temporarily shut down in August 2014 owing to a large *Microcystic* bloom in the lake (Steffen et al., 2017).

Besides well-known cyanobacterial toxins (e.g. microcystin, cylindrospermopsin etc.) that are passively released from dying cells (decline growth phase), many cyanobacteria produce other harmful secondary metabolites which differ from cyanobacterial toxins and which also cause ecological problems (Harke et al., 2016; Sukenik et al., 2015; Esther et al., 2014; Leflaive and Ten-Hage, 2007). These secondary metabolites suppress other phytoplankton (Wang et al., 2017; Żak et al., 2012; Suikkanen et al., 2004; Keating, 1978), disrupt germination and seedling growth of submerged macrophytes (Xu et al., 2016, 2015; Zheng et al., 2013), affect the fitness, protein expression and genetic structure of zooplankton (Drugă et al., 2016; Lyu et al., 2016; Zagatto et al., 2012; Lampert, 2010), influence behavior, survivorship and population of fishes (Hamilton et al., 2014; Zagatto et al., 2012), and may include teratogenic and estrogenic effects both in fish and amphibians (Smutná et al., 2017; Jonas et al., 2015, 2014; Sychrová et al., 2012).

In addition, previous studies demonstrated that adversely effects of cyanobacterial extracellular exudates are stronger than intracellular

---

extracts, and that these effects are growth phase-dependent. Extracellular exudates of decline phase cyanobacteria do not exhibit obvious negative effects (Xu et al., 2015), whereas extracellular exudates in exponential phase do affect coexisting organisms (Xu et al., 2016, 2015; Zheng et al., 2013; Žak et al., 2012; Suikkanen et al., 2004). Thus, it appears that the exponential phase is the critical period for cyanobacteria to produce secondary metabolites. Though accumulating evidence demonstrates that cyanobacteria exudate substances are harmful to aquatic organisms, the effect of exudates from exponential phase cells on aquatic animals remains unclear.

Fish are integral components of most aquatic ecosystems and may be threatened by secondary metabolites in waterbodies hosting blooms. (Godlewska et al., 2016; Sinden and Sinang, 2016). *Sinocyclocheilus grahami* (Barbinae subfamily) is an endemic species of the Yunnan-Guizhou plateau, and once dominated Dianchi Lake (24°51′-N, 102°42′-E) – the sixth largest lake in China – prior to its eutrophication. The species disappeared from the lake during the 1980s and is listed in the "China Red Data Book of Endangered animals (fish)" as a nationally protected animal (Chu and Chen, 1989). Many efforts have been made to rehabilitate *S. grahami* in the lake and in captivity. In 2007, the Endangered Fish Conservation Center (EFCC) achieved reproduction of *S. grahami* in captivity (Yang et al., 2007). More than one million larvae have been re-introduced to the lake since 2009, though these efforts have failed to rebuild the population.

Cyanobacteria blooms have become an increasingly serious problem in Dianchi Lake since the 1980s, and we hypothesize that they may be responsible for the disappearance of important fishes, including *S. grahami*, as well as its failed re-introduction into the lake. To test this hypothesis, we exposed *S. grahami* to exudates from the *Microcystis aeruginosa* grown in exponential phase, assessing embryo development using both phenotype and proteomics. Proteomics has informed our understanding of organism responses to stresses at the cellular level, as many protein functions and responses can be assessed simultaneously. Although proteomics approaches have been used previously to reveal impacts of cyanobacterial on Daphnia (Lyu et al., 2016), and fish embryo toxicity (FET) screening in whole-effluent testing has been standardized (Lammer et al., 2009), this is the first study to assess phenotype and protein responses in fish exposed to cyanobacteria exudates.

2. Materials and methods

2.1. *M. aeruginosa cultivation and exudates (MaE) production*

M. aeruginosa (FACHB-905, toxic) that originated from Dianchi Lake was obtained from the Freshwater Algae Culture Collection of the Institution of Hydrobiology (FACHB-Collection) at the Chinese Academy of Sciences, and was cultured in a axenically-modified HGZ-145 nutrient solution. Preparation of the nutrient solution and culture methods and conditions are described in Zheng et al. (2013). Cultures were grown in a climate-controlled room (GXZ-380B, China) at 25 ± 1 °C in a 12:12 h light-dark cycle to the exponential phase, and manually shaken twice daily. Cyanobacteria cells were counted manually by hemocytometer with an optical microscope (Olympus, BX51, Japan) to obtain an initial inoculation density of $1.2 - 1.4 \times 10^6$ cells/ml. *M. aeruginosa* cells were harvested after 3-d growth and a homogenized culture used to achieve a density between 4.0 and 4.5×10^6 cells/ml in HGZ-145 solution by centrifugation for 10 min at 11,000 rpm. Supernatant was filtered through a glass-fiber filter (0.22 μm) (MiLiMo separation technology limited company, Shanghai) to obtain the original MaE solution.

2.2. *S. grahami embryos obtained and gamete quality assessment*

Adult *S. grahami* fish were obtained from Kunming Institute of Zoology, Chinese Academy of Sciences. Spawning are induced by injection Luteinizing Hormone Releasing Hormone (LHRH-A2) and

Table 1
Quality evaluation standard of gametes of *S. grahami*.

Indicator	Mean $\pm$ SD
Egg	
Egg size (mm)	2.3 ± 0.2
Semi-diameter of yolk sac (mm)	1.9 ± 0.1
Nuclear deviation rate%	92.0 ± 3.0
Sperm	
Sperm motility (%)	93.0 ± 3.0
Duration of sperm forward movement (s)	22.0 ± 1.0
Duration of sperm movement (s)	70.0 ± 3.0

Domperidone (DOM) (Pan et al., 2014). As the quality of embryos depends on the quality of gametes, we evaluated the latter before artificial insemination to ensure all embryos used in this experiment were healthy (see Table 1). Specifically, we measured egg size (mm), semi-diameter of yolk sac (mm), and nuclear deviation rate (ND, %; ND is an indicator that can forecast fertilization rate). Sperm motility (%) (Mounib, 1978), duration of sperm forwards movements, and sperm lifespan(s) were also measured.

2.3. The effect of MaE on S. grahami embryos and sperm

We exposed sperm/embryos that were obtained by artificial insemination (dry method of artificial fertilization) to varying concentrations of MaE in petri-dishes (see Table 2). Concentrations of MaE to which sperm/embryos were exposed were well within the natural range. The sperm motility (%) and sperm lifespan (s) have been measured. In total, 50 embryos were exposed in 40 ml culture solution and replicated three times (treatments and controls). Petri-dishes were incubated at 18 ± 1 °C. We assessed development of embryos during five periods: cleavage, blastula, gastrula, segmentation, and hatching. Fertilization rate was measured after the gastrula period. Hatchability and mortality rate were measured when 90% of embryos had hatched. Malformation rate was measured across the entire hatching period. Development of embryos, malformation level evaluation, and post-embryonic development were monitored under a stereoscope from 1 h post-fertilization (hpf), and the duration time of each development period and growth characteristics were recorded. Abnormal embryos were photographed and dead embryos (apparent as loose and milky yolk) were removed every $3 - 4$ h to maintain growth medium quality.

2.4. Proteomics analysis

Control and experimental embryos (30% MaE) were used in a proteomics analysis. According to preliminary research, malformations of embryos were the most obvious symptom of MaE exposure, and malformation rates the most important sub-lethal indicator, thus we chose samples that exhibited significant malformation for proteomics analysis. In this study, exposure to 50% MaE induced the highest malformation rates, but was too toxic to obtain sufficient embryo samples and malformation types. Thus, we chose embryos exposed to < 30% MaE for proteomic analysis. We collected samples when the eyes of

Table 2
Treatment concentrations of *Microcystis aeruginosa* exudates (MaE).

Original MaE cell density (cells/ml)	Percent of original MaE solution (%)		Algae density of Treatment concentration of MaE (cells/ml)
4×10^6 cells/ml	control	0	0
	Low concentration	10	0.4×10^6
	Medium	30	1.2×10^6
	concentration	50	2×10^6
	High concentration	100	4×10^6

Table 3
Mean (± SD) effect of MaE exposure on duration of embryonic development stage. * $P < 0.05$ (compared with control).

Stage of embryonic development	Duration time of embryonic development (h)				
	Control	10%	30%	50%	100%
Fertilization (s)	30	30	30	30	30
Cleavage					
Blastodisc	1.4 − 1.7	1.4 − 1.7	1.4 − 1.7	1.4 − 1.7	1.4 − 1.7
2–32cells	6 − 6.5	6 − 6.5	6 − 6.5	6 − 6.5	6 − 6.5
Blastula	18 ± 1.1	17.8 ± 2.0	17.7 ± 1.7	17.4 ± 1.2*	15.5 ± 0.8*
Gastrula	23.3 ± 1.0	23.4 ± 1.5	23.4 ± 1.1	23.5 ± 2.0	23.4 ± 0.6
Segmentation	50 ± 0.8	50 ± 0.9	50 ± 1.0	50 ± 1.2	50 ± 1.0
Hatching	60 ± 3.2	57.8 ± 4.5	63.8 ± 3.0*	51.4 ± 3.5*	50.7 ± 3.0*
Hatching time (h)	158.7 ± 2.1	156.4 ± 1.34*	162.2 ± 2.4*	149.7 ± 5.3*	146.9 ± 4.9*
Accumulated temperature (°C/h)	2936.1 ± 5.7	2892.5 ± 6.0*	3000.3 ± 5.5*	2768.9 ± 6.7*	2718.0 ± 6.9*

embryos turned black as the time node (hatching period). Approximately 80–100 embryos from both controls (no MaE exposure) and treatments were placed into cryogenic vials with a latex dropper, tinfoil wrapped, and then stored in liquid nitrogen at −80 °C.

Cell pellets were suspended on ice in 200 μl lysis buffer (4% SDS, 100 mM DTT, 150 mM Tris-HCl pH 8.0), and boiled for 5 min. Samples were then ultrasonicated and boiled for another 5 min. Undissolved cellular debris was removed by centrifugation at 14,000 rpm for 15 min. The supernatant was collected and quantified with a BCA Protein Assay Kit (Bio-Rad, USA). Digestion of protein (250 μg for each sample) was performed according to the FASP procedure described by Wiśniewski et al. (2009). The peptide content was estimated by UV light spectral density at 280 nm.

The peptide portion of each sample was desalted on C18 Cartridges (Empore™ SPE Cartridges C18 (standard density), bed I.D. 7 mm, volume 3 ml, Sigma), then concentrated by vacuum centrifugation and reconstituted in 40 μl of 0.1% (v/v) trifluoroacetic acid. Liquid Chromatography (LC)-Electrospray Ionization (ESI) Tandem MS (MS/MS) Analysis was performed on a Q Exactive mass spectrometer that was coupled to Easy nLC (Proxeon Biosystems, now Thermo Fisher Scientific). Five μg of peptide was loaded onto a C18-reversed phase column (Thermo Scientific Easy Column, 10 cm long, 75 μm inner diameter, 3 μm resin) in buffer A (2% acetonitrile and 0.1% Formic acid) and separated with a linear gradient of buffer B (80% acetonitrile and 0.1% Formic acid) at a flow rate of 250 nL/min controlled by IntelliFlow technology over 120 min. MS data was acquired using a data-dependent top10 method dynamically choosing the most abundant precursor ions from the survey scan (300–1800 m/z) for HCD fragmentation. Determination of the target value was based on predictive Automatic Gain Control (pAGC). Dynamic exclusion duration was 25 s. Survey scans were acquired at a resolution of 70,000 at m/z 200 and resolution for HCD spectra was set to 17,500 at m/z 200. Normalized collision energy was 30 eV and the underfill ratio, which specifies the minimum percentage of the target value likely to be reached at maximum fill time, was defined as 0.1%. The instrument was run with peptide recognition mode enabled. MS experiments were performed in triplicate for each sample.

MS data was analyzed using MaxQuant software version 1.3.0.5. MS data were searched against the UniProtKB *Escherichia coli* database (2585998 total entries, downloaded 06/07/12). An initial search was set at a precursor mass window of 6 ppm. The search followed an enzymatic cleavage rule of Trypsin/P and allowed a maximum of two missed cleavage sites and a mass tolerance of 20 ppm for fragment ions. Carbamidomethylation of cysteines was defined as fixed modification, while protein N-terminal acetylation and methionine oxidation were defined as variable modifications for database searching. The cutoff of global false discovery rate (FDR) for peptide and protein identification was set to 0.01. Label-free quantification was carried out in MaxQuant (Schwanhäusser et al., 2011). Intensity-based absolute quantification (iBAQ) in MaxQuant was performed on the identified peptides to quantify protein abundance.

2.5. Data analysis

Fertilization rate (μ_1) and mortality rate (μ_2) were calculated as:

$$\mu_1 = N_1/N_0 \cdots\cdots\cdots \tag{1}$$

$$\mu_2 = N_2/N_0 \cdots\cdots\cdots \tag{2}$$

where N_1 and N_2 were the number of live embryos remaining after gastrulation and dead embryos after all embryo hatched, respectively, and N_0 is initial embryo number (50 eggs). Hatchability rate (μ_3) and malformation rate (μ_4, μ_5) were respectively calculated as:

$$\mu_3 = N_3/N \cdots\cdots\cdots \tag{3}$$

$$\mu_4 = N_4/N \cdots\cdots\cdots \tag{4}$$

where N_3 is hatching larvae, N_4 is malformed embryos, N is fertilized embryos.

$$\mu_5 = N_5/N_4 \cdots\cdots\cdots \tag{5}$$

where N_5 is the number of larvae suffered different malformation category (yolk sac malformation, thoracic deformity, spinal curvature, multi-malformation and other malformation type), with this formula used in Table 3 only.

Accumulated temperature (K) was calculated as K = T·n, where T is the average culture temperature and n is culture duration (h). Data were expressed as mean ± standard deviation. We used one-way analysis of variance (ANOVA) and subsequent post-hoc tests (Fisher LSD) to examine differences in all tests by using SPSS 19.0 after checking for normality and homoscedasticity.

3. Results

Fertilization rate and hatching rate decreased, while malformation rate and mortality rate increased, with increasing MaE concentration for exposed *S. grahami* embryos (Fig. 1A–D, respectively). Fertilization rate declined progressively from 67.5% in controls to 53.6%, 54.3%, 45.8% and 35.4% with 10%, 30%, 50% and 100% MaE exposure, respectively ($P < 0.01$) (Fig. 1A). Likewise, hatching rate declined from 84.3% in controls with healthy larvae to 15.5% in 100% MaE exposure ($P < 0.01$) (Fig. 1B). Though embryos successfully hatched in 100% MaE exposure, larvae were unhealthy and inactive. Conversely, embryo malformation rates increased with increasing MaE concentration between 10% and 50% MaE exposure, but declined thereafter (Fig. 1C). Strong teratogenic effects on embryos were apparent at even the lowest MaE exposure concentration (10%). Malformation rate in this group increased to 27.6% versus 16.6% in controls ($P < 0.05$). We observed the highest malformation rate (39.3%) at the 50% MaE concentration ($P < 0.01$). Paradoxically, malformation rate was lower (24.2%) when
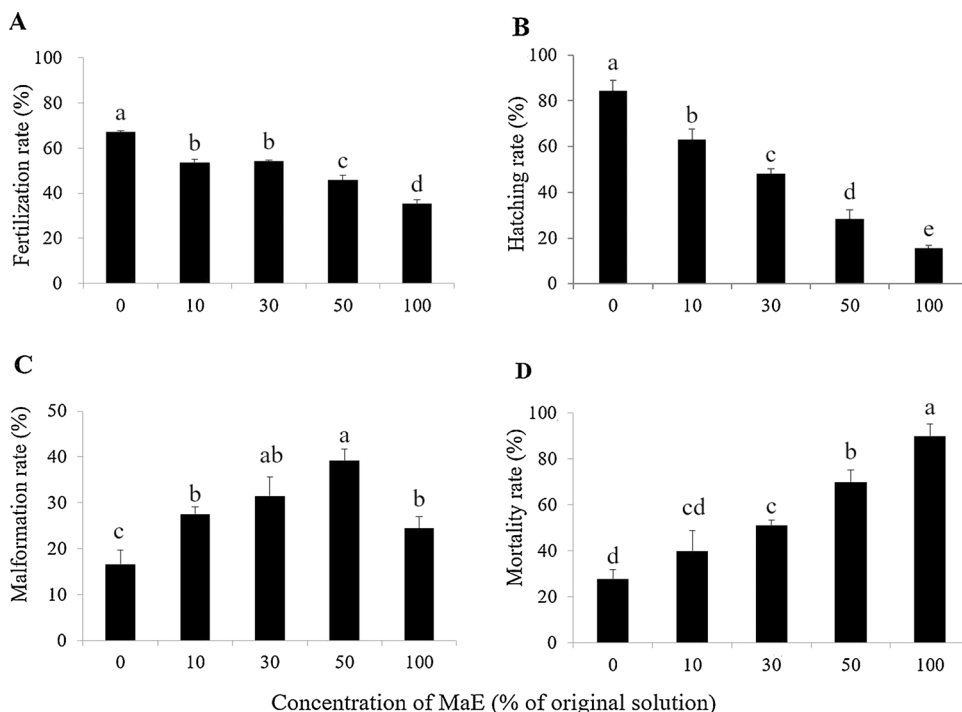
A

B

C

D

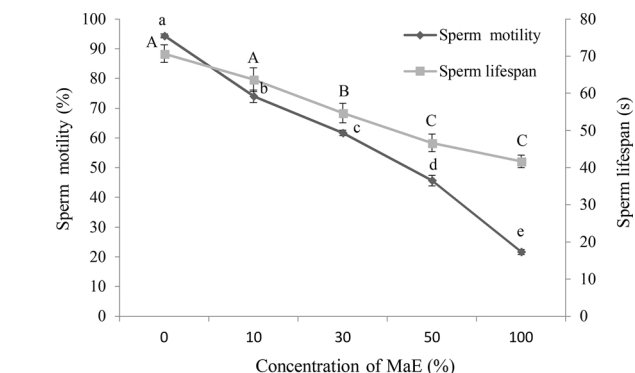Concentration of MaE (% of original solution)

Fig. 2. Mean (+standard deviation) effects of *Microcystis aeruginosa* exudate (MaE) exposure on *S. grahami* sperm motility and lifespan. Significantly different groups are indicated by different letters above the bars.

embryos were exposed to the highest MaE concentration (100%), though their mortality rate was high. Mortality rate (90.0%) of embryos exposed to 100% MaE was significantly higher than that in controls (27.8%; P < 0.01) (Fig. 1D).

Sperm can be activated in all MaE concentration exposed, but the sperm motility are strongly affected by MaE. Sperm motility declined progressively from 94.3% in controls to 74.0%, 61.7%, 45.7% and 21.7% with 10%, 30%, 50% and 100% MaE exposure, respectively (P < 0.01) (Fig. 2). Sperm lifespan also shortened under MaE

exposure, which decline from 71.7 s in controls to 63.7s, 54.67s, 46.67 s and 41.67 s with 10% (P > 0.05), 30%, 50% and 100% (P < 0.01) MaE exposure, respectively.

Embryonic development started after 1.4 h post-fertilization (hpf); the duration of the cleavage period was 6 h for treatments exposed to MaE, which was similar to controls (Table 3). The blastula period increased with increasing MaE concentration, with developmental times for 10–50% MaE exposure and control groups all > 17 h, while at the highest dose (100%) it was truncated to 15.5 h (P < 0.01) (Table 3). Duration time of the hatching period peaked at 30% MaE exposure (~4 h longer; P < 0.05), while those at concentrations of 10, 50 (P < 0.01) and 100% (P < 0.01) MaE were all shorter than in controls (Table 3).

Fish embryo malformations were wide-ranging in individuals exposed to MaE exudates. However, the type and degree of malformations differed under different MaE exposures (Table 4; Fig. 3). Malformed embryos ranged from mild to serious impairment when exposed to MaE exudates (Fig. 3). Impairments included yolk sac malformation, thoracic deformity, spinal curvature, and multi-malformations, among others (Fig. 3). Yolk sac malformation decreased progressively with increasing MaE concentration (P < 0.01), from a high of 61.0% in controls to 10.3% at 100% MaE exposure (Table 4). Thoracic deformities were elevated only at lower concentrations of MaE (10, 30%; P < 0.05) (Table 4). Spinal curvature malformations were highest at these same MaE concentrations (P < 0.05), but were elevated in all MaE treatments (Table 4). Multi-malformations were elevated but

Table 4
Mean (± SD) malformation rates for *S. grahami* embryos in different malformation categories under different MaE concentration exposures. All malformation rates under different MaE concentration exposures were compared with control values. * P < 0.05.

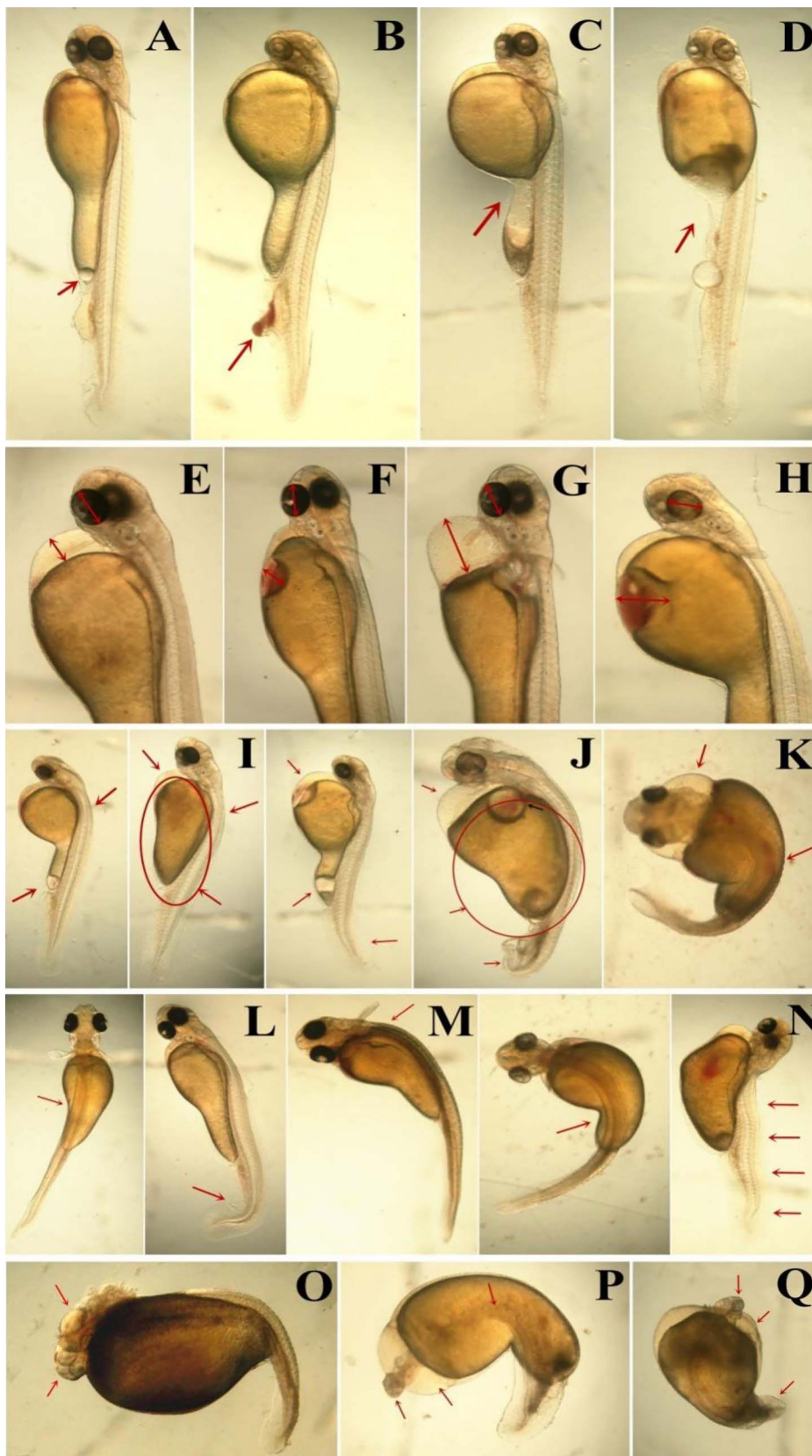| Malformation type	Concentration of MaE (%)				
	Control	10	30	50	100
Yolk sac malformation	61.0 ± 3.1	31.5 ± 3.8*	20.0 ± 1.3*	14.3 ± 0.6*	10.3 ± 1.6*
Thoracic deformity	15.0 ± 2.2	23.0 ± 2.0*	21.9 ± 1.0*	16.7 ± 0.4	14.7 ± 2.2
Spinal curvature	12.8 ± 1.1	24.6 ± 0.4*	25.4 ± 1.3*	19.6 ± 1.8	18.7 ± 3.1
Multi-malformation	11.2 ± 0.7	20.9 ± 2.0*	32.7 ± 2.5*	43.1 ± 2.6*	51.9 ± 1.9*
Other malformation type	–	–	3.5 ± 1.8	6.2 ± 1.9	4.5 ± 2.2

Fig. 3. Control (A & E) and malformed embryos of *S. grahami* under MaE-stress. Malformed larvae include yolk sac malformation (B–D), thoracic deformity (F–H), spinal curvature (I–K), multi-malformations (L–N), and other malformation types including double head (O), encephalatrophy (P), and axon shortened (Q). Abnormalities are highlighted with red arrows. (For interpretation of the references to colour in this figure legend, the reader is referred to the web version of this article.)

proportional to MaE concentration (Table 4). Particularly severe malformations such as double-head and encephalatrophy occurred only at moderate to high MaE concentrations (i.e. ≥ 30%). In general, we observed that severity of deformities increased from low MaE

concentrations to higher ones.

After-hatch larvae exposed to MaE typically experienced one or more of three typically developmental deficiencies: swollen pericardium; spinal curvature often accompanied with swollen
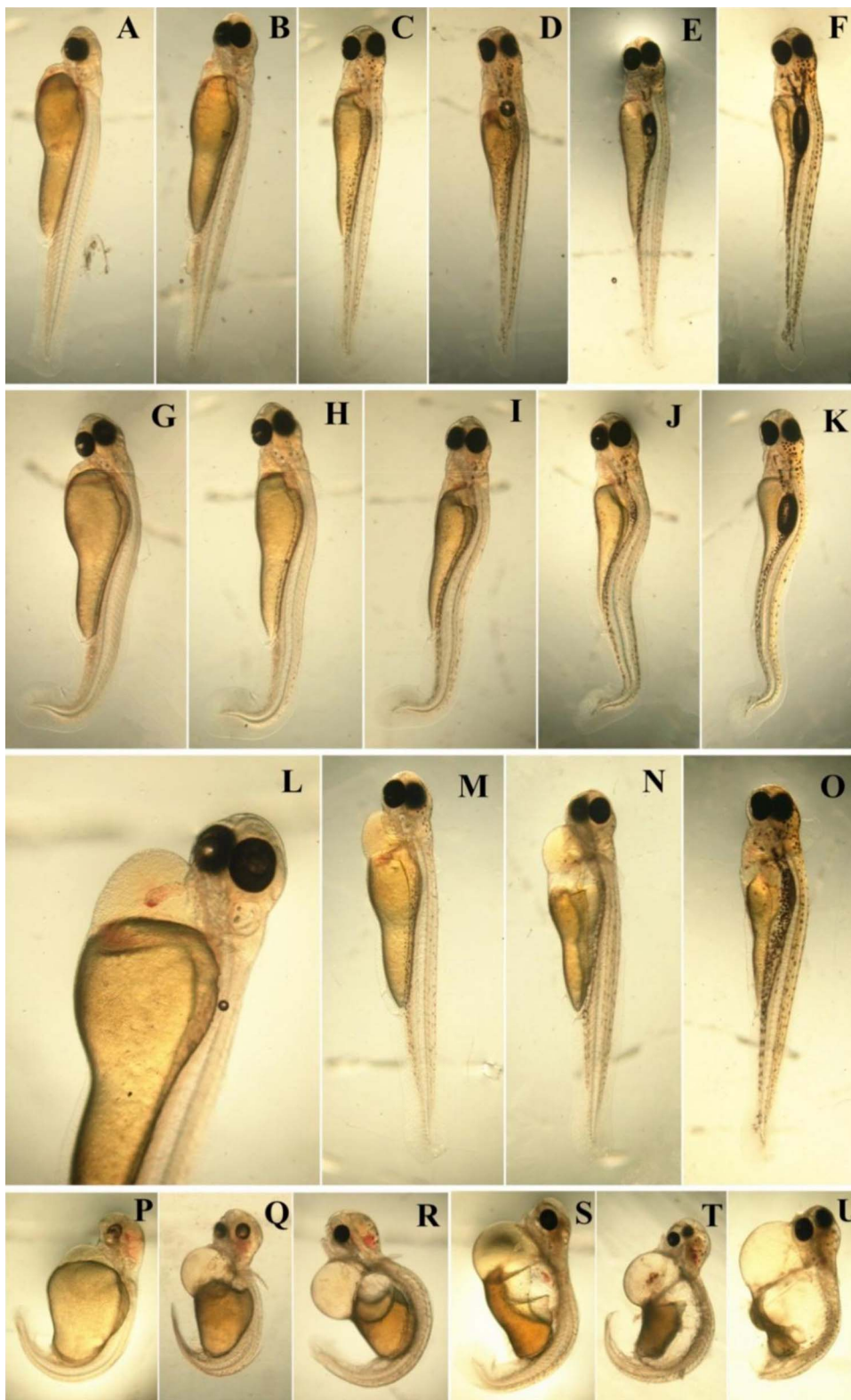
Fig. 4. Development process of after-hatched larvae of *S. grahami* exposed to MaE. The development process of normal (control) larvae (A–F), and those with spinal curvature (G–K), thoracic deformity (L–O), or multi-malformation (P–U).

pericardium; or death of fry within one month and without organ development. MaE-exposed developing fry exhibited a swollen pericardium (Fig. 4L–0) or multi-malformations (Fig. 4P–U) between days 1 and 10, while those lacking developed organs are highlighted in Fig. 4P–U. The progression of development of spinal curvature for fry aged 1–9 d is highlighted in Fig. 3G and K, respectively. Both normal fry (Fig. 4U) and malformed fry (Fig. 4J) could develop a functional and

healthy swim bladder by 7 d.

We explored all proteins that were over/under-expressed (by at least 2-fold/0.5 times) or which could only be detected in controls or treatments when exposed to MaE exudates. In total, there are 1112 proteins expression in MaE-treated *S. grahami* embryos were significantly changed (318 differentially expressed proteins, 742 and 52 proteins were detected in control and treatment, respectively). Further
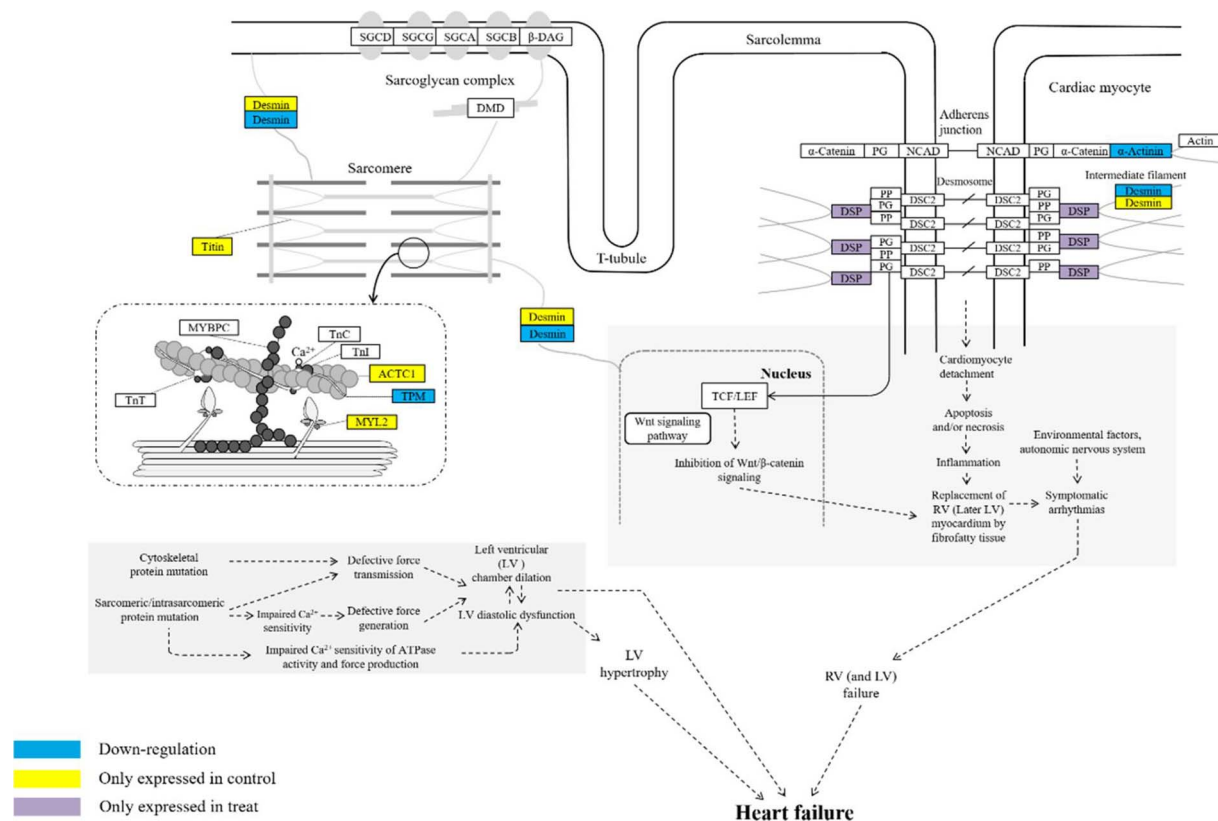
Fig. 5. Pathway of MaE-induced cardiac abnormality in fish embryos.

gene ontology (GO) annotations and pathway analysis were performed, and 1680 GO terms and 288 pathways were involved. Phenotype observations indicated that larvae suffered very serious heart dysplasia. Complementary proteomic analysis revealed that MaE could strongly alter expression of two proteins that are closely associated with heart systoly and diastoly. Protein S100A1 was over-expressed 26 times as compared to the control, while myosin light chain was under-expressed 25-fold. Both proteins are related to calcium ion balance. Further KEGG (Kyoto Encyclopedia of Genes and Genomes) study revealed that MaE also influenced the structure of cardiac sarcomere and cardiomyocyte (Fig. 5), which ultimately lead to ventricular hypertrophy.

4. Discussion

Our previous research demonstrated that secondary metabolites (other than microcystins) produced from exponential-exudates-phase cells adversely affected green algae, diatoms, and macrophytes by inhibiting growth and photosynthesis (Wang et al., 2017; Xu et al., 2016, 2015; Zheng et al., 2013). This study extends these effects to animals. Both embryo and sperm assays demonstrated that MaE has strong adverse effects on fish. Successful survival of offspring is a key requirement of population establishment, persistence or recovery. The failure of embryo development when exposed to MaE could be a major obstacle to successful reintroduction of this fish species in Dianchi Lake. Field studies of reintroduced *S. grahami* across six years indicate that larvae can survive and grow to sexual maturity in Dianchi Lake, but a subsequent generation has never been found. Results of our study indicate that negative effects associated with MaE exposure are consistent with demographic failure of this species in the lake.

Using both phenotype and proteomic expression, our study revealed a broad array of adverse responses by individuals exposed to MaE, ranging from coarse phenotype malformations to altered proteome. Among the consequences, the most noteworthy is the teratogenic effect of MaE. Teratogenic effects are now known to impact *S. grahami*, other

fish species (i.e. zebra fish), and amphibians (Jaja-Chimedza et al., 2017; Smutná et al., 2017; Jonas et al., 2015, 2014). These findings indicate possible ubiquitous effects of MaE exposure, and even a potential risk to mammals including humans. Observation of post-embryonic development of larvae demonstrated that teratogenicity of exudates may have profound consequences. For example, teratogenic larvae exhibited no organ development with time (see Fig. 4P–U). Considering the complexity of this developmental process, it is, however, difficult to identify the mechanisms responsible for this phenomenon.

Heart failure seems to be an unavoidable consequence of MaE exposure based on our combined phenotypic observations and proteomic analysis. The shape of the larva's heart becomes long and narrow under MaE exposure (fig. 4L) as compared with controls animals (fig. 4A). Proteomic analysis then demonstrated aberrant expression in both cardiac structural proteins and proteins related to cardiac systole function. Notable among them is S100A1, a regulator of myocardial contractility, which was overexpressed 26-fold. S100A1 belongs to S100 protein family, which is the largest subfamily of EF-hand Ca^{2+}-binding proteins. S100A1 overexpression would enhance cardiac contractile performance both by regulating sarcoplasmic reticulum Ca^{2+} handling and myofibrillar Ca^{2+} responsiveness (Most et al., 2001). S100A1 could increases Ca^{2+} release from the sarcoplasmic reticulum by interacting with the ryanodine receptor (Ehlermann et al., 2000), which in turn would lead to an imbalance of Ca^{2+} flux. Conversely, S100A1 also has the potential to rescue *in vivo* cardiac function after acute myocardial infarction as well as in chronic heart function, as this protein has anti-hypertrophic and anti-apoptotic properties (Most et al., 2007). Hence, further studies should be carry out to examine whether increased S100A1 protein content yields overall beneficial or detrimental effects with respect to heart failure in developing embryos.

Exposures to MaE caused earlier hatching compared to controls, an effect previously observed in zebra fish embryos under cyanobacterial extract exposure (Jonas et al., 2015). This effect is probably associated

with some unknown compounds produced by cyanobacteria.

Additional study is required to identify other sub-lethal effects (such as endocrine disruption; estrogenic effect) associated with MaE exposure, and the underlying mechanisms responsible for these patterns. Moreover, evaluation of MaE ecological hazards, and the management of water pollution, should consider unknown or unclear responses by natural biota to cyanobacteria toxins. Hazard assessment should include an evaluation/early-warning system based on molecular responses considering their sensitivity and the importance of water aquatic biota and humans.

5. Conclusion

We conclude that *Microcystis aeruginosa* can significantly affect fish embryos by exudates from exponential phase cells. Our experiments revealed strong teratogenic and lethal effects of *M. aeruginosa* on the development of an endangered fish embryo, apparently the result of heart disease. Future tests on allelopathic effects of *M. aeruginosa* should take toxic exudates into account.

Acknowledgements

References

Barda, I., Kankaanpää, H., Putina, I., Balode, M., Sjövall, O., Meriluoto, J., 2015. Bioaccumulation of hepatotoxins-a considerable risk in the Latvian environment. Environ. Pollut. 196, 313–320.

Bengis, R., Govender, D., Lane, E., Myburgh, J., Oberholster, P., Buss, P., Prozesky, L., Keet, D., 2016. Eco-epidemiological and pathological features of wildlife mortality events related to cyanobacterial bio-intoxication in the kruger National Park, South Africa. J. South Afr. Vet. Assoc. 87, 1–9.

Chu, X.L., Chen, Y.R., 1989. The Fishes of Yunnan China-Part I Cyprinidae. Beijing, Science Press, pp. 1–377.

Drugă, B., Turko, P., Spaak, P., Promati, F., 2016. Cyanobacteria affect fitness and genetic structure of experimental *Daphnia* populations. Environ. Sci. Technol. 50, 3416–3424.

Ehlermann, P., Remppis, A., Guddat, O., Weimann, J., Schnabel, P.A., Motsch, J., Heizmann, C.W., Katus, H.A., 2000. Right ventricular upregulation of the ca^{2+} binding protein S100A1 in chronic pulmonary hypertension. Biochim. Et Biophys. Acta Mol. Basis Dis. 1500, 249–255.

Esther, K., Verena, G., Daniel, H., Rainer, K., Karl, G., Jakob, P., Judith, B., 2014. The toxicity and enzyme activity of a chlorine and sulfate containing aeruginosin isolated from a non-microcystin-producing Planktothrix strain. Harmful Algae 39, 154–160.

Godlewska, M., Izydorczyk, K., Kaczkowski, Z., Jóźwik, A., Długoszewski, B., Ye, S., Lian, Y.X., Guillard, J., 2016. Do fish and blue-green algae blooms coexist in space and time? Fish. Res. 173, 93–100.

Gong, W.D., Browne, J., Hall, N., Schruth, D., Paerl, H., Marchetti, A., 2017. Molecular insights into a dinoflagellate bloom. ISME J. 11, 439–452.

Hamilton, T.J., Paz-Yepes, J., Morrison, R.A., Palenik, B., Tresguerres, M., 2014. Exposure to bloom-like concentrations of two marine *Synechococcus* cyanobacteria (strains CC9311 and CC9902) differentially alters fish behaviour. Conserv. Physiol. 2, 1–9.

Harke, M.J., Steffen, M.M., Gobler, C.J., Otten, T.G., Wilhelm, S.W., Wood, S.A., Paerl, H.W., 2016. A review of the global ecology, genomics, and biogeography of the toxic cyanobacterium, *Microcystis* spp. Harmful Algae 54, 4–20.

Jaja-Chimedza, A., Sanchez, K., Gantar, M., Gibbs, P., Schmale, M., Berry, J.P., 2017. Carotenoid glycosides from cyanobacteria are teratogenic in the zebrafish (*Danio rerio*) embryo model. Chemosphere 174, 478–489.

Jonas, A., Buranova, V., Scholz, S., Fetter, E., Novakova, K., Kohoutek, J., Hilscherova, K., 2014. Retinoid-like activity and teratogenic effects of cyanobacterial exudates. Aquat. Toxicol. 155, 283–290.

Jonas, A., Scholz, S., Fetter, E., Sychrova, E., Novakova, K., Ortmann, J., Benisek, M., Adamovsky, O., Giesy, J.P., Hilscherova, K., 2015. Endocrine, teratogenic and neurotoxic effects of cyanobacteria detected by cellular in vitro and zebrafish embryos assays. Chemosphere 120, 321–327.

Keating, K.I., 1978. Blue-green algal inhibition of diatom growth: transition from mesotrophic to eutrophic community structure. Science 199, 971–973.

Lammer, E., Carr, G.J., Wendler, K., Rawlings, J.M., Belanger, S.E., Braunbeck, T., 2009. Is the fish embryo toxicity test (FET) with the zebrafish (*Danio rerio*) a potential alternative for the fish acute toxicity test? Comp. Biochem. Physiol. Part C Toxicol.

Pharmacol. 149, 196–209.

Lampert, W., 2010. Laboratory studies on zooplankton-cyanobacteria interactions. N. Z. J. Mar. Freshw. Res. 21, 483–490.

Leflaive, J., Ten-Hage, L., 2007. Algal and cyanobacterial secondary metabolites in freshwaters: a comparison of allelopathic compounds and toxins. Freshw. Biol. 52, 199–214.

Lopez-Rodas, V., Maneiro, E., Lanzarot, M.P., Perdigones, N., Costas, E., 2008. Mass wildlife mortality due to cyanobacteria in the Donana National Park. Spain Vet. Rec. 162, 317–318.

Lyu, K., Meng, Q.G., Zhu, X.X., Dai, D.X., Zhang, L., Huang, Y., Yang, Z., 2016. Changes in iTRAQ-based proteomic profiling of the cladoceran *Daphnia magna* exposed to microcystin-producing (MP) and microcystin-free (MF) *Microcystis aeruginosa*. Environ. Sci. Technol. 50, 4798–4807.

Most, P., Bernotat, J., Ehlermann, P., Pleger, S.T., Reppel, M., Börries, M., Niroomand, F., Pieske, B., Janssen, P.M.L., Eschenhagen, T., Karczewski, P., Smith, G.L., Koch, W.J., Katus, H.A., Remppis, A., 2001. S100a1: a regulator of myocardial contractility. Proceedings of the National Academy of Sciences of the United States of America 98, 13889–13894.

Most, P., Remppis, A., Pleger, S.T., Katus, H.A., Koch, W.J., 2007. S100a1: a novel inotropic regulator of cardiac performance. Transition from molecular physiology to pathophysiological relevance. Am. J. Physiol. Regul. Integr. Comp. Physiol. 293, 568–577.

Mounib, M.S., 1978. Cryogenic preservation of fish and mammalian spermatozoa. J. Reprod. Fertil. 53, 13–18.

Paerl, H.W., Paul, V.J., 2012. Climate change: links to global expansion of harmful cyanobacteria. Water Res. 46, 1349–1363.

Paerl, H.W., Gardner, W.S., McCarthy, M.J., Peierls, B.L., Wilhelm, S.W., 2014. Algal blooms Noteworthy nitrogen. Science 346, 175–176.

Paerl, H.W., Huisman, J., 2008. Blooms like it hot. Science 320, 57–58.

Pan, X.F., Wang, X.A., Ma, L., Li, Z.Y., Chen, X.Y., Yang, J.X., 2014. Artificial fertilization and embryonic development of *Sinocyclocheilus grahami* (Regan) from dianchi lake China. Biodivers. Bioprospect. Dev. 1, 1–6.

Schwanhäusser, B., Busse, D., Li, N., Dittmar, G., Schuchhardt, J., Wolf, J., Chen, W., Selbach, M., 2011. Global quantification of mammalian gene expression control. Nature 473, 337–342.

Sinden, A., Sinang, S.C., 2016. Cyanobacteria in aquaculture systems: linking the occurrence, abundance and toxicity with rising temperatures. Environ. Sci. Technol. 13, 1–8.

Smutná, M., Priebojová, J., Večerková, J., Hilscherová, K., 2017. Retinoid-like compounds produced by phytoplankton affect embryonic development of *Xenopus laevis*. Ecotoxicol. Environ. Saf. 138, 32–38.

Steffen, M.M., Davis, T.W., McKay, R.M.L., Bullerjahn, G.S., Krausfeldt, L.E., Stough, J.M.A., Neitzey, M.L., Gilbert, N.E., Boyer, G.L., Johengen, T.H., Gossiaux, D.C., Burtner, A.M., Palladino, D., Rowe, M.D., Dick, G.J., Meyer, K.A., Levy, S., Boone, B.E., Stumpf, R.P., Wynne, T.T., Zimba, P.V., Gutierrez, D., Wilhelm, S.W., 2017. Ecophysiological examination of the lake erie *Microcystis* bloom in 2014 linkages between biology and the water supply shutdown of toledo. OH Environ. Sci. Technol. 51, 6745–6755.

Stewart, I., Seawright, A.A., Shaw, G.R., 2008. Cyanobacterial poisoning in livestock, wild mammals and birds − an overview. Adv Exp. Med. Biol. 619, 613–637.

Suikkanen, S., Fistarol, G.O., Granéli, E., 2004. Allelopathic effects of the Baltic cyanobacteria *Nodularia spumdigena, Aphanizomenon flos-aquae* and *Anabaena lemmermannii* on algal monocultures. J. Exp. Mar. Biol. Ecol. 308, 85–101.

Sukenik, A., Quesada, A., Salmaso, N., 2015. Global expansion of toxic and non-toxic cyanobacteria: effect on ecosystem functioning. Biodiver. Conserv. 24, 889–908.

Sychrová, E., Štěpánková, T., Nováková, K., Bláha, L., Giesy, J.P., Hilscherová, K., 2012. Estrogenic activity in extracts and exudates of cyanobacteria and green algae. Environ. Int. 39, 134–140.

Testai, E., Scardala, S., Vichi, S., Buratti, F.M., Funari, E., 2016. Risk to human health associated with the environmental occurrence of cyanobacterial neurotoxic alkaloids anatoxins and saxitoxins. Crit. Rev. Toxicol. 46, 1–35.

Visser, P.M., Verspagen, J.M.H., Sandrini, G., Stal, L.J., Matthijs, H.C.P., Davis, T.W., Paerl, H.W., Huisman, J., 2016. How rising CO_2 and global warming may stimulate harmful cyanobacterial blooms. Harmful Algae 54, 145–159.

Wang, L.C., Zi, J.M., Xu, R.B., Hilt, S., Hou, X.L., Chang, X.X., 2017. Allelopathic effects of *Microcystis aeruginosa* on green algae and a diatom: evidence from exudates addition and co-culturing. Harmful algae 61, 56–62.

Wiśniewski, J.R., Zougman, A., Nagaraj, N., Mann, M., 2009. Universal sample preparation method for proteome analysis. Nat. Methods 6, 359–362.

Xu, R.B., Wu, F., Hilt, S., Wu, C., Wang, X.L., Chang, X.X., 2015. Recovery limitation of endangered *Ottelia acuminata* by allelopathic interaction with cyanobacteria. Aquat. Ecol. 49, 333–342.

Xu, R.B., Hilt, S., Pei, Y., Yin, L.J., Wang, L.C., Chang, X.X., 2016. Growth phase-dependent allelopathic effects of cyanobacterial exudates on *Potamogeton crispus L.* seedlings. Hydrobiologia 767, 137–149.

Yang, J.X., Pan, X.F., Li, Z.Y., 2007. Preliminary report on the successful breeding of the endangered fish *Sinocyclocheilus grahami* endemic to dian chi lake. Zool. Res. 28, 329–331.

Żak, A., Musiewicz, K., Kosakowska, A., 2012. Allelopathic activity of the Baltic cyanobacteria against microalgae. Estuar. Coast Shelf Sci. 112, 4–10.

Zagatto, P.A., Buratini, S.V., Aragão, M.A., Ferrão-Filho, A.S., 2012. Neurotoxicity of two *Cylindrospermopsis raciborskii* (cyanobacteria) strains to mice, Daphnia, and fish. Environ. Toxicol. Chem. 31, 857–862.

Zheng, G.L., Xu, R.B., Chang, X.X., Hilt, S., Wu, C., 2013. Cyanobacteria can allelopathically inhibit submerged macrophytes: effects of *Microcystis aeruginosa* extracts and exudates on *Potamogeton malaianus*. Aquat. Bot. 109, 1–7.